[Journal of Geophysical Research – Atmosphere]

Supporting Information for

A comprehensive study about the in-cloud processing of nitrate through coupled measurements of individual cloud residuals and cloud water

Guohua Zhang[1,2,3], Xiaodong Hu[1,2,4], Wei Sun[1,2,4], Yuxiang Yang[1,2], Ziyong Guo[1,2,4], Yuzhen Fu[1,2], Haichao Wang[5], Shengzhen Zhou[5], Lei Li[6], Mingjin Tang[1,2,3], Zongbo Shi[7], Duohong Chen[8], Xinhui Bi[1,2,3,*], Xinming Wang[1,2,3]

[1] State Key Laboratory of Organic Geochemistry and Guangdong Provincial Key Laboratory of Environmental Protection and Resources Utilization, Guangzhou Institute of Geochemistry, Chinese Academy of Sciences (CAS), Guangzhou 510640, PR China

[2] CAS Center for Excellence in Deep Earth Science, Guangzhou, 510640, China

[3] Guangdong-Hong Kong-Macao Joint Laboratory for Environmental Pollution and Control, Guangzhou Institute of Geochemistry, CAS, Guangzhou 510640, PR China

[4] University of Chinese Academy of Sciences, Beijing 100049, PR China

[5] School of Atmospheric Sciences, Sun Yat-sen University, Guangzhou 519082, PR China

[6] Institute of Mass Spectrometer and Atmospheric Environment, Jinan University, Guangzhou 510632, PR China

[7] School of Geography, Earth and Environmental Sciences, University of Birmingham, Birmingham B15 2TT, U.K.

[8] State Environmental Protection Key Laboratory of Regional Air Quality Monitoring, Guangdong Environmental Monitoring Center, Guangzhou 510308, PR China

Contents of this file

Text S1-S3

Table S1

Figures S1 to S7

Introduction

Details including the analysis of air masses, meteorological conditions, and characteristics of individual particles over the sampling periods. Text describes the lifetime calculation for NOx and N_2O_5, and regression and random forest analysis of nitrate production. Tables provide the initial setup of model simulations for nitrate formation in aqueous phase (wet aerosol and cloud droplets). Figures mainly show the characteristics of individual particles, including representative mass spectra and the RPA ratios (nitrate/sulfate) for the identified particle types, distribution of nitrate RPA over cloud free, interstitial, and residual particles, and also the comparison of [NOx][O3] and SA between cloud events and cloud-free periods.

Text S1 Lifetimes of NOx and N_2O_5

The formation of nitrate from hydrolysis of N_2O_5 arises from the reactions between NO_2 and O_3 can be given as follows:

$NO_2 + O_3 \rightarrow NO_3 + O_2$ (R1)

$NO_2 + NO_3 + M \rightarrow N_2O_5 + M$ (R2)

Thus, NOx is converted to N_2O_5 at the following rate ($K_1 = 1.2\times10^{-13}$ exp (-2450/T), T is the absolute temperature), and thus the lifetime of NOx can be calculated as:

$$\tau_{NO_x} = \frac{1}{2K_1[O_3]}$$

During daytime, NO_3 rapidly photolyzes, but at night, NO_3 reacts with NO_2 to produce N_2O_5. The key reaction to produced condensed nitrate is the hydrolysis of N_2O_5 on aerosol or droplet surfaces:

$N_2O_5 + H_2O \rightarrow 2HNO_3$ (R3)

The reaction proceeds effectively on the surface of aerosol particles that contain water. When an N_2O_5 molecule strikes the surface of an aqueous particle, not every collision leads to reaction. A reaction efficiency or uptake coefficient γ was introduced to account for the probability of reaction. Values of γ for this reaction ranging from 0.06 to 0.1 have been reported. The the lifetime of N_2O_5 can be calculated as:

$$\tau_{N_2O_5} = \left[\frac{\gamma}{4}\left(\frac{8RT}{\pi m_{(N_2O_5)}}\right)^{1/2} A_p\right]^{-1}$$ (Seinfeld and Pandis, 2006)

where $\left(\frac{8RT}{\pi m_{(N_2O_5)}}\right)^{1/2}$ corresponds to the molecular mean speed of N_2O_5, $m_{(N_2O_5)}$ is the molecular mass of N_2O_5, and A_p is the aerosol/droplet surface area (SA) per unit volume ($cm^2\ cm^{-3}$). The reaction occurs at a rate governed by that at which N_2O_5 molecules strike the aerosol surface area times the amount of surface area times the reaction efficiency.

58

59 **Text S2 Regression and random forest analysis**

60 As shown in Test S1, the formation of nitrate depends on the [NOx][O_3], SA, and
61 temperature as inputs, and thus could be roughly regressed as follows:

62 Nitrate ~ exp(-1/T) $[O_3][NO_2]\ T^{1/2}A_p$

63 In the multiple linear model, the least-squares fit is used, and two of the most common
64 measures of model fit are the residual standard error and the proportion of variance
65 explained (R^2). It is noted that A_p (or SA) is not available and thus was not included in the
66 regression for 2018 spring data.

67 Random forest analysis, is for nonlinear multiple regression, using trees as building
68 blocks to construct powerful prediction models [*Breiman*, 2001]. The algorithm first
69 creates multiple decision trees, where each tree is grown by using the bootstrap re-sampling
70 method. The relative importance of the predictor variables can also be obtained, with
71 "Mean Decrease Accuracy" presenting the capability of each independent variable in
72 explaining the variability of SNRs.

73

74 **Text S3 SPAMS**

75 Individual particles are introduced into the SPAMS through a critical orifice. They are
76 focused and accelerated to specific velocities, which can be determined by two continuous
77 diode Nd:YAG laser beams (532 nm) placed downstream. Based on the measured
78 velocities, a pulsed laser (266 nm) is subsequently triggered to desorp/ionize the particles.
79 The generated positive and negative molecular fragments are recorded. The measured
80 velocities are corresponding to d_{va}, based on a calibration using polystyrene latex spheres

(PSL, Duke Scientific Corp., Palo Alto) with predefined sizes (0.15-2.0 μm). Peak thresholds were set to record only those peaks with area greater than 5 units to distinguish peaks from the background noise (< 1 unit) in the mass spectra.

TABLES

Table S1. The initial setup of model simulations for nitrate formation in aqueous phase (wet aerosol and cloud droplets)

In wet aerosol and cloud droplet the RH, LWC, and radius are different, in wet aerosol case: RH=85% , LWC1=1.0×10^{-5} g/m^3， LWC2= 1.0×10^{-4} g/m^3, radius of aerosol particles is 0.5 μm; in cloud droplet case: RH=99.99%, LWC1= 0.05 g/m^3, LWC2= 0.15 g/m^3, radius of aerosol particles is 8 μm, and photolysis rate was changed 100%, 50%, and 30%.

	Wet aerosol	**Wet aerosol**	**Cloud 1#**	**Cloud 2#**
RH	85%	85%	100%	100%
LWC (g cm^{-3})	10^{-5}	10^{-4}	0.05	0.15
Radius (μm)	0.5	0.5	8	8
NO_2 (ppb)	25	25	25	25
O_3 (ppb)	100	100	100	100
photolysis rate (%)	100	100	100; 50; 30	100; 50; 30

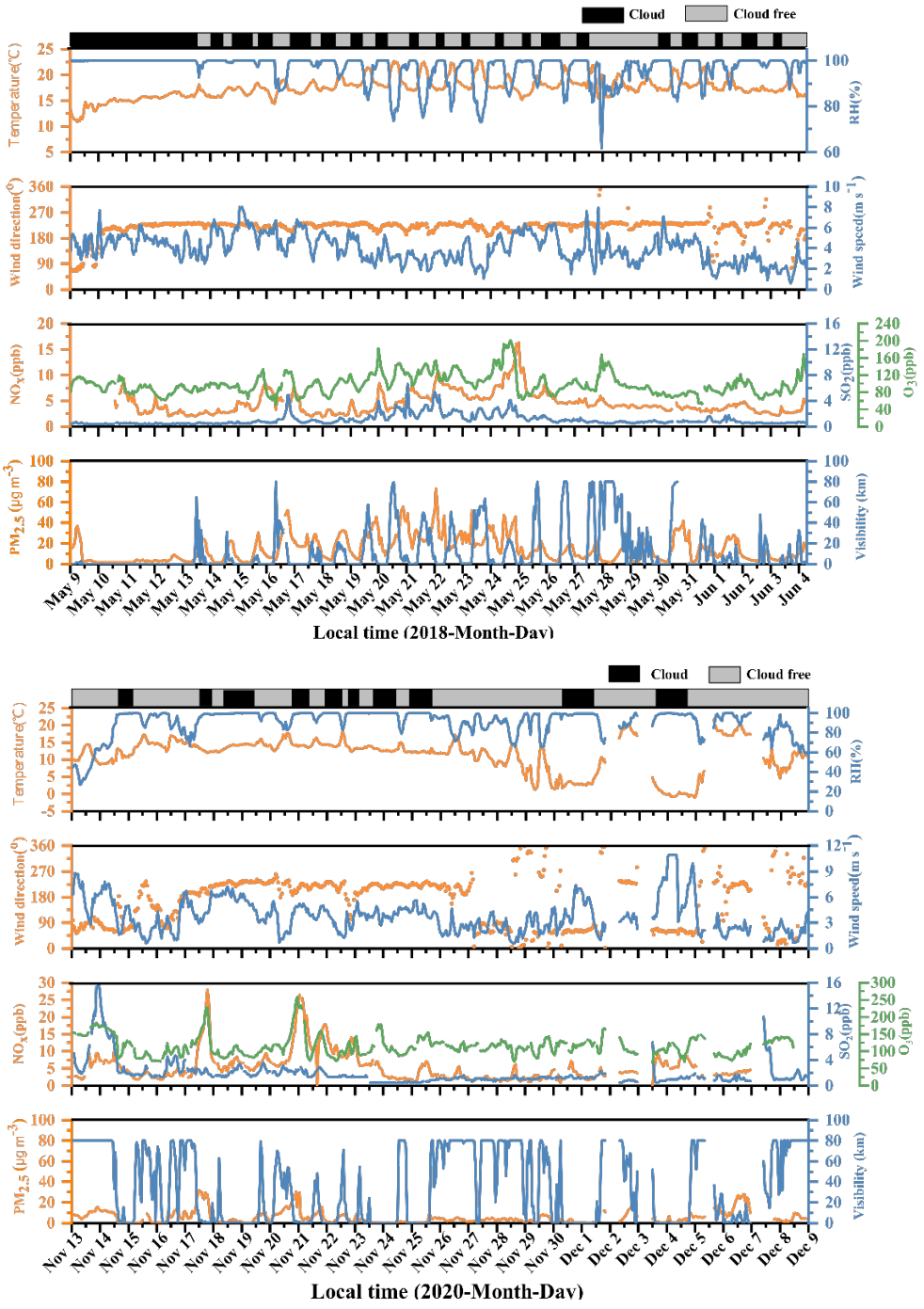

93

94 **Figure S1.** Temporal variations of T and RH, wind speed and direction, O_3/SO_2/NO_x, and

95 mass concentration of $PM_{2.5}$ and visibility for 2018 spring (upper) and 2020 winter

96 (bottom), respectively.

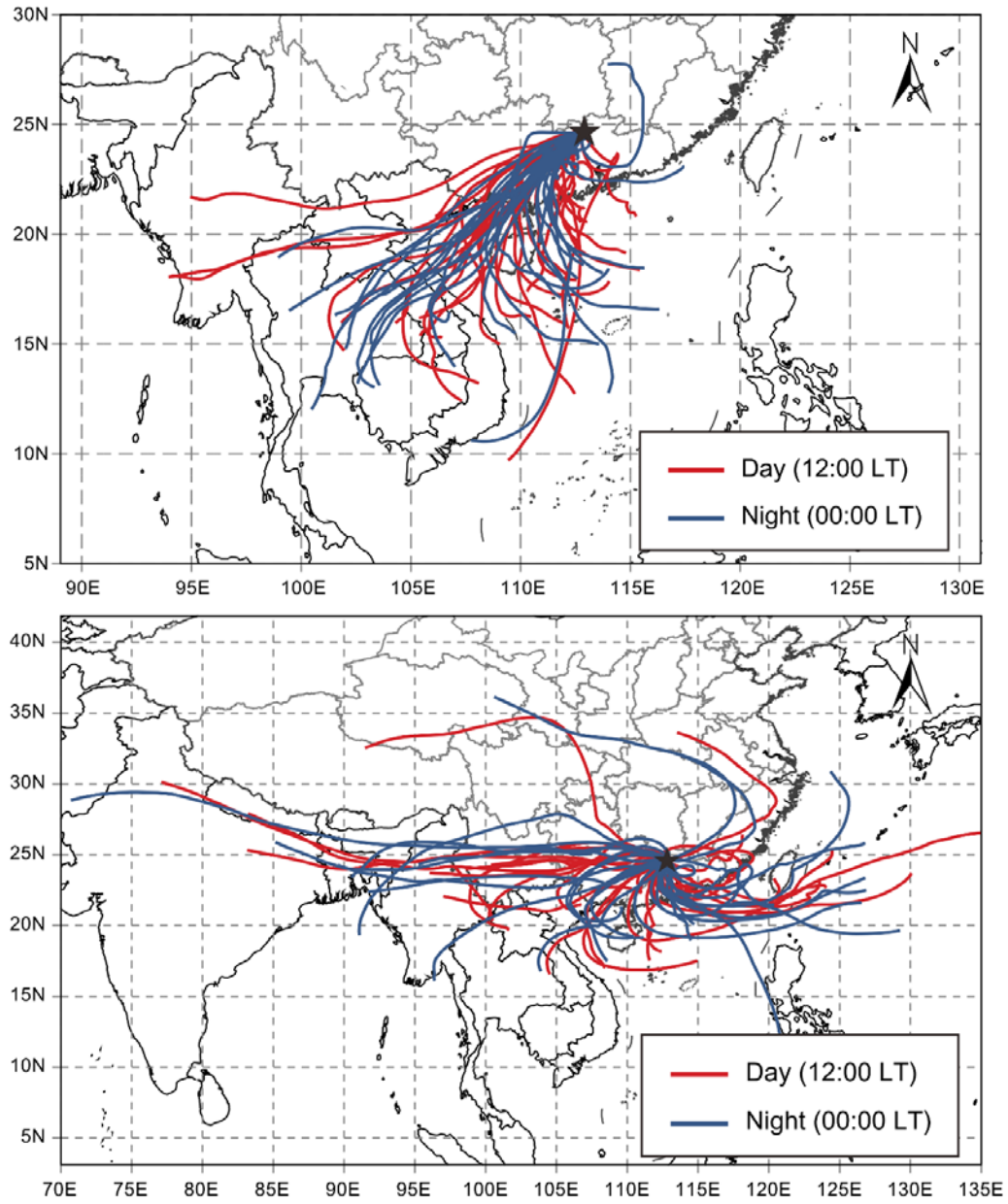

97

98 **Figure S2.** The HYSPLIT back trajectories (72 h) arriving at the sampling site (100 m
99 above the sea level) at daytime (12:00 local time, left panel) and nighttime (0:00 local time,
100 right panel) for 2018 spring (upper) and 2020 winter (bottom), respectively.

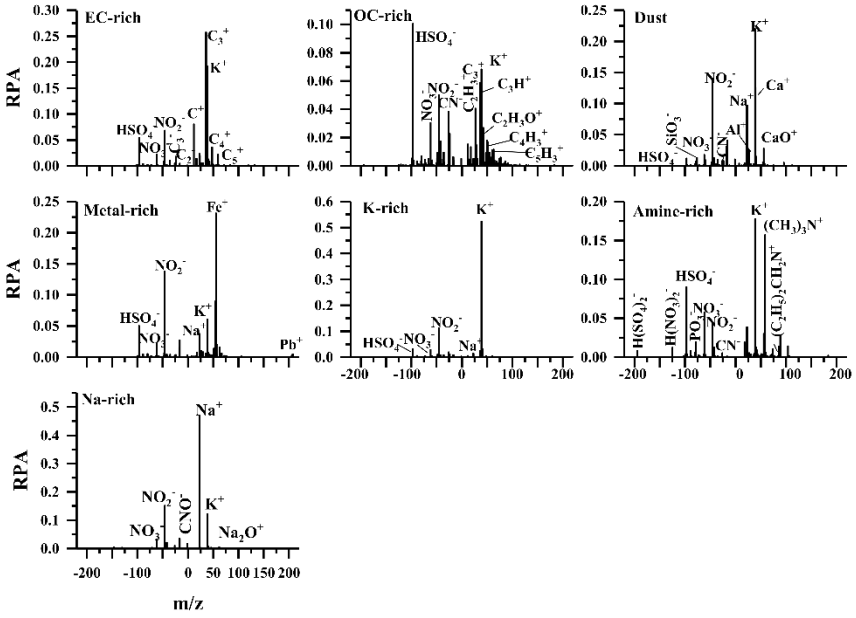

Figure S3. Representative mass spectra for the identified particle types. Each particle type is labeled according to the most significant chemical features in the mass spectra. In addition to the presence of secondary inorganic species (i.e., sulfate (-97[HSO_4].$^-$), nitrate (-62[NO_3]$^-$), and ammonium (18[NH_4]$^+$)), the mass spectrum of the OC-rich particles is mainly contributed by OC markers (37[C_3H]$^+$, 50[C_4H_2]$^+$, 51[C_4H_3]$^+$, 55[C_4H_7]$^+$ and 63[C_5H_3]$^+$); EC-rich by both EC ion peak clusters ([C_n]$^{+/-}$, n = 1, 2, 3, …); K-rich particles by intense potassium peak (39[K]$^+$); Sea salt by 23[Na]$^+$, 39[K]$^+$, and chloride (-35[Cl]$^-$ and -37[Cl]$^-$); Amine-rich by [$N(CH_3)_3$]$^+$ and [$(C_2H_5)_2N(CH_3)$]$^+$; Dust by 27[Al]$^+$ and 40[Ca]$^+$; Metal-rich by 23[Na]$^+$, 39[K]$^+$, 56[Fe]$^+$ and 206-208[Pb]$^+$.

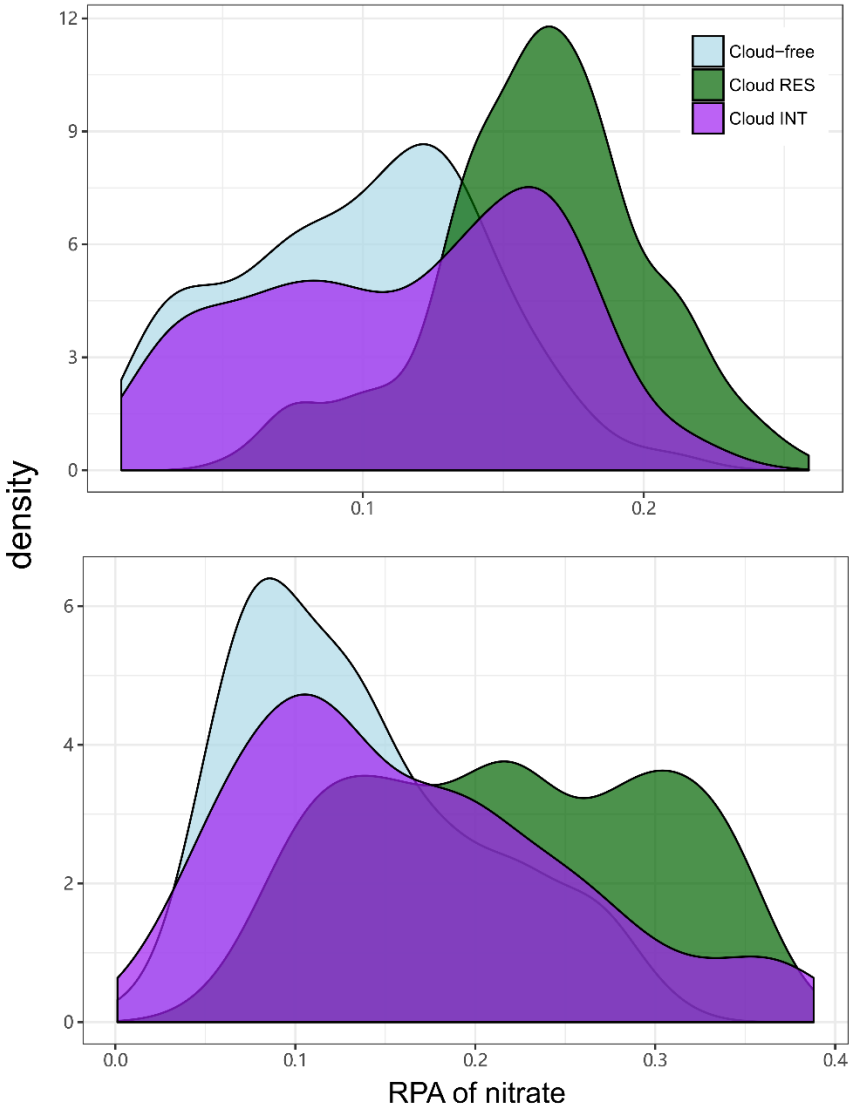

Figure S4. Distribution of RPA of nitrate, separated for cloud free, INT, and RES particles, in 2018 spring (upper) and 2020 winter (bottom).

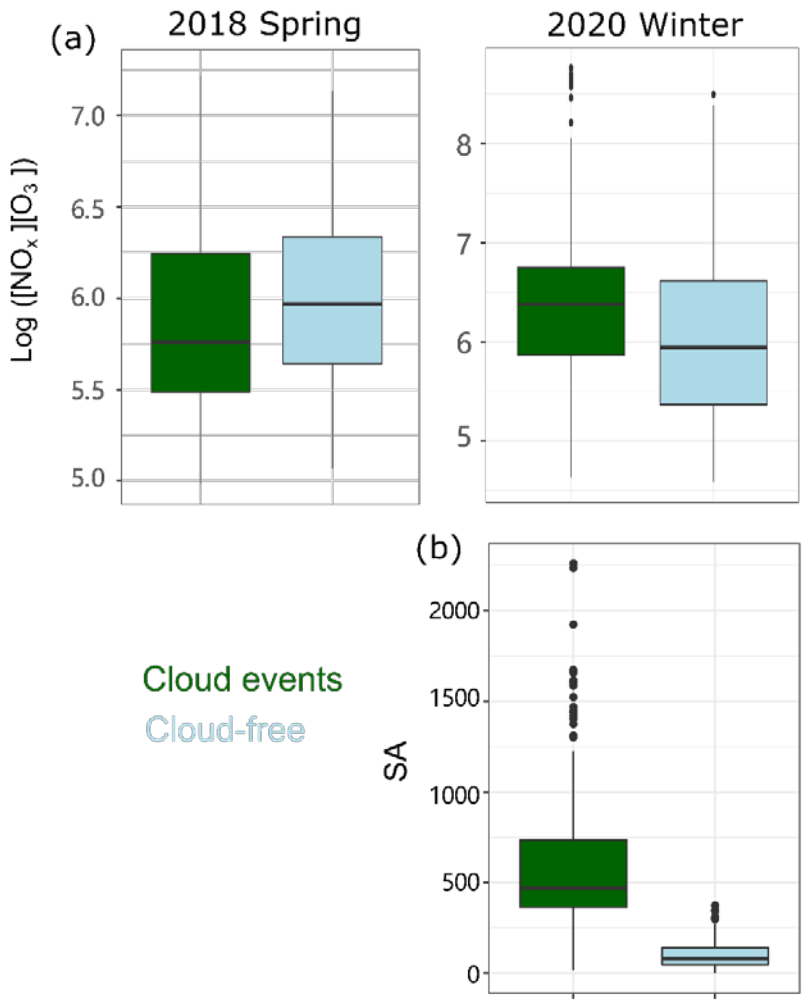

115

116 **Figure S5.** Box-and-whisker plots of [NOx][O_3] and SA (μm^2 cm^{-3}) during cloud

117 events and cloud-free periods in (a) 2018 spring and (b) 2020 winter, respectively.

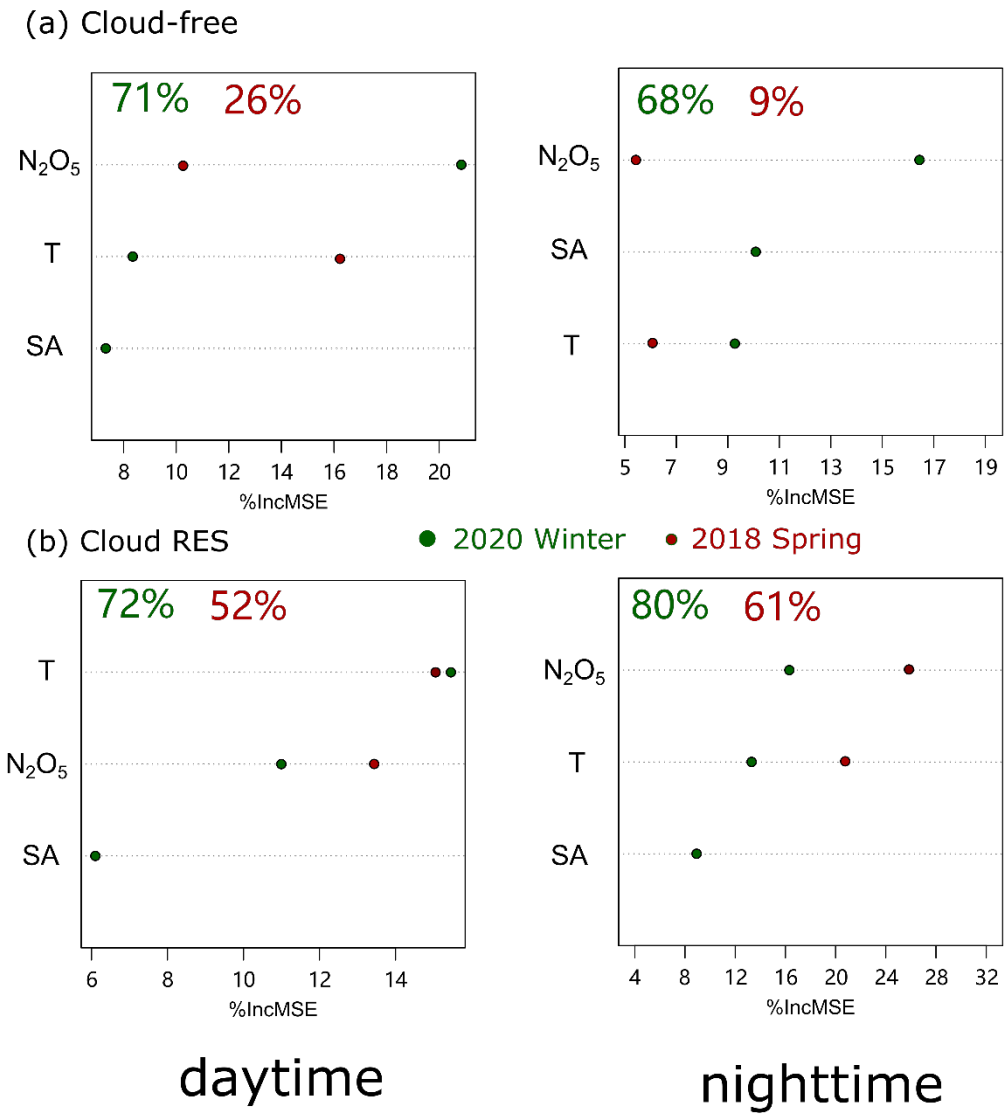

Figure S6. The relative importance of predictors in the random forest analysis for the RPA of nitrate associated with the (a) cloud-free particles and (b) cloud residual particles, respectively, separated for daytime and nighttime during 2018 spring and 2020 winter. Used as an indicator for the relative contribution to the predicted variable, %IncMSE refers to the increased mean square-error when each independent variable is removed from the predictors.

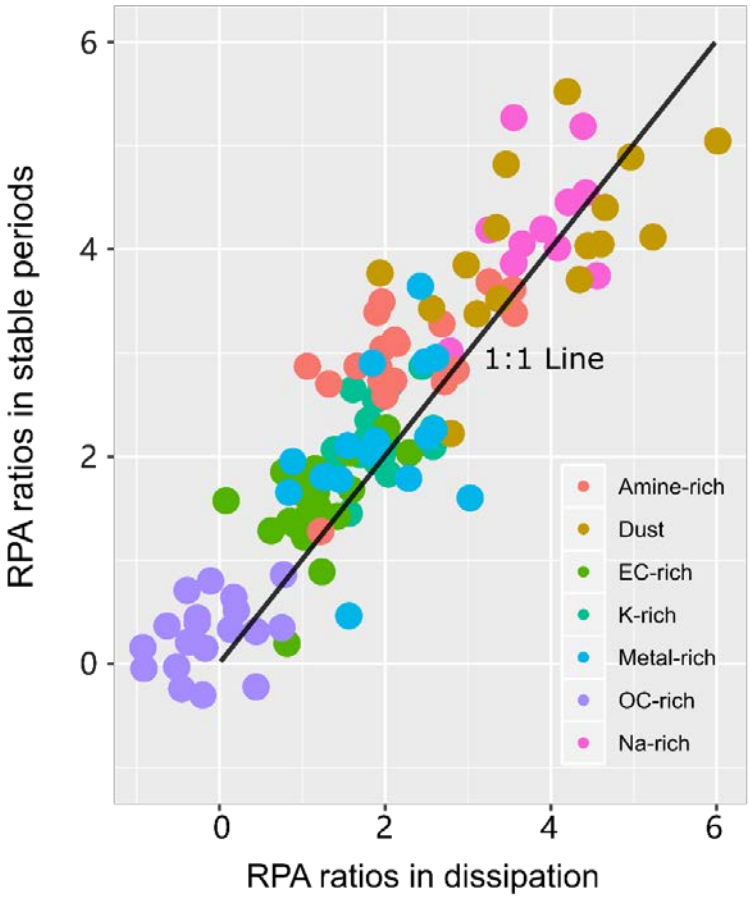

Figure S7. The RPA ratios (nitrate/sulfate) varying on the seven single particle types are compared for mid-cloud and cloud dissipation periods (2h after cloud period) for 2018 spring, which is also similarly observed in 2020 winter. The RPA ratios during cloud dissipation periods generally follows those in the cloud RES particles during cloud stable periods. It suggests that the in-cloud produced nitrate remains after cloud evaporation. It is anticipated that the evaporation of the cloud droplets in the ambient atmosphere would lead to a level similar to the cloud RES nitrate, and perhaps more if the ambient relative humidity were higher or the temperature lower than that in the GCVI (Hayden et al., 2008). As the GCVI is a more severe and rapid approach to the

drying of cloud droplets than likely occurs in the atmosphere, the enhanced cloud residual nitrate suggests that when the cloud evaporates, more particulate nitrate than existed in the aerosol below cloud should be released into the air. If this process is significant, an enhancement of nitrate (relative to sulfate) may be expected after cloud evaporation.